X-ray Calorimeters

Caroline K. Stahle

NASA / Goddard Space Flight Center, Laboratory for High Energy Astrophysics, Greenbelt, MD, 20771

Motivation

The 0.1 – 10 keV x-ray band corresponds to temperatures from 10^6 to 10^8 K. At these temperatures, the primary radiation is emitted in photo- and collisionally-excited characteristic lines of partially ionized heavy elements. These lines allow us to diagnose the elemental abundances and physical conditions in the gas, and measurements of Doppler shifts and line widths can give valuable information about motion. (The richness of x-ray astronomy is discussed in detail elsewhere in these proceedings[1].) Naturally, in order to be of any use, these spectral lines must be resolvable.

Grating spectrometers are capable of high spectral resolution, and Chandra and XMM are now putting this technology to good use. The good energy resolution of grating spectrometers requires optics with very high angular resolution, but the design of x-ray telescopes has involved a trade-off between angular resolution and collecting area, putting gratings at a sensitivity disadvantage. Gratings disperse a spectrum across a position sensitive detector, but if the source is extended, the position and spectral information can be difficult to disentangle. For these reasons, a means for measuring x-ray spectra non-dispersively, but with high resolution, was sought.

How is energy measured? This very simple question must be answered before discussion of direct detectors for use as spectrometers can commence. Let us divide direct energy detectors into two categories: non-equilibrium and equilibrium. In a non-equilibrium detector, the more familiar of the two, the absorbed energy produces quantized excitations, each with energy much greater than kT. These are counted to determine the energy. Since, invariably, some of the energy goes elsewhere, such as into heat, the ultimate energy resolution is determined by the statistics governing the partition of energy between the system of excited states and everything else. This is how most photon and particle detectors work.

Since loss of energy to heat limits the resolution of a non-equilibrium detector, one might reason that better resolution would be attainable in a detector that allows all the energy to be manifested as heat. This is an equilibrium detection scheme. The energy is deposited in an isolated thermal mass and the resulting increase in temperature is measured. At the time of the measurement, all of the deposited energy has become heat and the sensor is in thermal equilibrium. The ultimate energy resolution is determined by how well one can measure this change in temperature against a background of thermodynamically unavoidable temperature fluctuations. This measurement of energy by measuring a change in temperature is known as calorimetry, an old technique made extremely powerful by the advent of milliKelvin refrigerators.

Foundations and unique considerations for x-rays

A calorimeter is conceptually a simple device[2]. As shown in Figure 1, it consists of a thermal mass to absorb the energy of incident radiation, a thermometer to measure the resulting temperature rise, and a weak link to a low-temperature heat sink that provides the thermal isolation needed for a temperature change to be sensed. Some basic principles are obvious from the outset. We need to operate at a low temperature so that the deposited energy is large relative to the random transfer of heat across the weak link that is required by statistical mechanics. We need a sensitive thermometer. We need the thermal link to be sufficiently weak that the thermal recovery time is the slowest time constant in the system (compared with thermalization and diffusion times), yet not so weak that the device can't handle the incident flux. We need an absorber appropriate to the radiation or particles to be detected. For x rays, we need an absorber that is opaque to x†rays yet has a low heat capacity so that a small deposition of energy is translated into a measurable temperature change. That absorber must thermalize well. Thermalization is the process by which the initially very non-equilibrium energy distribution at the instant of photo-electric absorption becomes an equilibrium distribution of energy than can be described by a temperature. The absorber must reproducibly and efficiently distribute the energy of the initial photon across a thermal distribution of phonons or electrons, depending on

the thermometer.

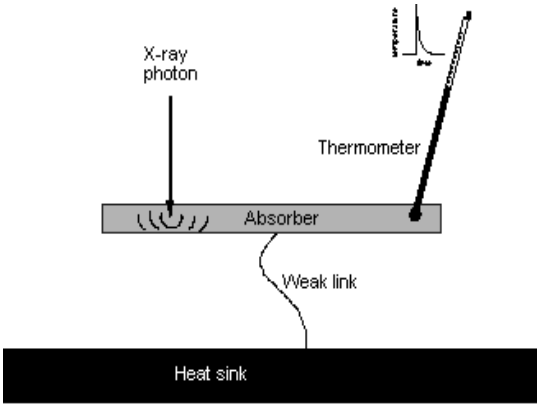

Figure 1

How well can a calorimeter measure the energy it absorbs? Consider a calorimeter with a thermometer that transduces changes in temperature into a voltage. It has a heat capacity C and a link with thermal conductance G to a heat sink. An instantaneous deposition of energy into the absorber will produce a voltage pulse with an exponential decay time constant t equal to C/G. The Fourier transform of the signal will be nearly independent of frequency f for f<<1/2pt and will fall off as 1/f above this corner frequency. The magnitude of the noise due to the random transfer of energy across the link to the heat sink (an elementary calculation in statistical mechanics) has the same frequency distribution as the signal. If this “phonon noise” were the only source of noise, the signal-to-noise ratio would be frequency-independent. Since the frequency components of the signal are correlated but those of the noise are independent and add in quadrature, the measurement error could be made arbitrarily small by employing a sufficiently large bandwidth. In reality, a frequency-independent noise term or a finite thermalization time will reduce the signal-to-noise ratio at high frequencies, effectively limiting the usable bandwidth. This is illustrated in Figure 2. This discussion of usable bandwidth assumes that an optimal digital filter is used. Each frequency bin of the signal is used to estimate the pulse height, weighted by the ratio of the signal to the noise power at that frequency.

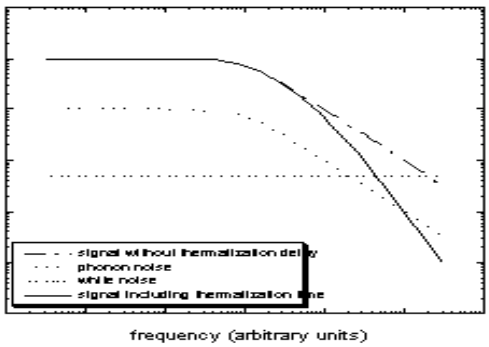

Figure 2

To understand the bandwidth limitations and calculate the highest energy resolution attainable, we need to consider specific implementations of the basic calorimeter concept. Devices have been developed using resistive, capacitive, inductive, paramagnetic, and electron-tunneling thermometers. The best energy resolution to date has been achieved with superconducting transition-edge sensors and semiconductor thermistors, both of which are resistance-based thermometers. Among the non-resistive thermometers, the magnetic calorimeters have demonstrated the best performance and have tremendous potential. This paper will discuss the fundamentals of ideal calorimeters and the physics and performance of their real-life implementations. The discussion will focus primarily on the resistive calorimeters, with the fundamentals of the magnetic calorimeters presented

later as a contrasting case.

Ideal calorimeters with resistive thermometers

In resistance-based calorimeters, the signal-to-noise at high frequencies is reduced by the Johnson noise associated with the resistance of the thermometer. Thus, the temperature sensitivity and the bandwidth-limiting noise originate in the same property of the sensor. The parameter $\alpha \equiv d\log R/d\log T$ is used to express the sensitivity of a resistance-based thermometer. Moseley and colleagues [4] calculated the energy resolution attainable in an ideal resistive thermometer with a given *C* and *a* operated at a temperature *T*, following the similar optimization done by Mather for infrared bolometers [5] . Their calculation, done in the limit of small signal *(a, C,* and *G* constant during the pulse), assumes that all noise sources apart from phonon noise and Johnson noise are negligible and that resistance is a function of temperature alone. For the case that the phonon noise is much greater than the Johnson noise at low frequencies, $\Delta E \propto T\sqrt{C/|\alpha|}$. Since this expression can be written as $\xi\sqrt{kT^2C}$, where *x*depends on *a*and the bias condition and *k* is Boltzmann's constant, it is tempting to compare it to $\sqrt{kT^2C}$, the RMS value of the energy fluctuations due to transfer of heat across the weak link. Though the latter value has been called the "thermodynamic limit", it is not a limit on the energy resolution of a microcalorimeter. The prefactor *x* can be < 1.

An interesting property of resistive thermometers is that the bias power changes as the resistance changes. Consider a thermistor with a negative *a* that is biased with a constant current *I*. As *T* increases, *R* will fall, causing $I^2 R$, the Joule power, to drop. This electrothermal feedback makes the pulse recovery time faster than the *C/G* expected in the absence of feedback. This effect can be very important in devices with large | *a*|. It doesn't change the intrinsic signal-to-noise anywhere, but it can be used to reduce the pulse decay time to close to the limiting thermalization time, making most efficient use of the available bandwidth.

Performance of real semiconductor and superconductor based calorimeters

Semiconductor thermistors

Semiconductors doped within the metal-insulator transition were the first thermometers used in x-ray calorimeters. At low temperatures, electrical conduction in such thermistors proceeds via thermally activated hopping of charge carriers between localized impurity states through a mechanism called variable range hopping (VRH)[6] . In VRH, the average hopping distance increases as the temperature is lowered. It becomes more probable for an electron to tunnel further to a site requiring less change in energy than to tunnel to a nearby site with a difference in energy large compared to that available in the spectrum of phonons. Doped crystalline semiconductors have a Coulomb gap in the density of states, which causes the VRH resistance to take the form $R = R_0 \exp\left(\sqrt{T_0/T}\right)$. T_0 is a constant that depends sensitively on the doping density. R_0 depends on the resistor geometry and only weakly on doping density. Both ion-implanted silicon and neutron transmutation doped (NTD) germanium [7] have been used successfully in x-ray calorimeters. An advantage of silicon is the existence of well-established micro-machining techniques that permit the fabrication of devices in which the active pixels and their links to the heat sink form a monolithic array. Reproducibility and uniformity of doping density have been the advantages of NTD germanium.

Two non-ideal effects that occur in semiconductor thermistors are a decrease in resistance with increasing bias power even at fixed temperature (non-Ohmic behavior) [8] and excess noise at low frequencies (1/*f*noise) [9] . These limit how small the thermistor can be made, and hence its contribution to the heat capacity, since both get worse as the thermistor is made smaller. These effects also limit T_0, since both worsen with decreasing doping density.

The non-Ohmic behavior can be modeled by assuming decoupling of the electrons from the crystal lattice, allowing the electron temperature to increase relative to that of the lattice. Though it is difficult to reconcile hot electrons with the isolated carriers of VRH, this model has been a useful empirical depiction. The non-Ohmic effects are qualitatively the same in doped Si and Ge; though the decoupling is worse in Ge, the

specific heat is lower by about the same factor. Thus, thermistors of Si and Ge with the same heat capacity and temperature sensitivity exhibit the same non-Ohmic behavior.

The 1/f noise, though, has been a particularly vexing problem for the ion-implanted Si. This noise has been the dominant factor limiting the energy resolution in silicon-based calorimeter arrays [10]. Until recently, the ion-implantation technique used to make the Si thermistors could only extend to depths of a few tenths of a micron, much thinner than typical NTD Ge thermometers. Truncation effects were considered the likely cause of the 1/f noise in these thermometers. Recently, a new technique that diffuses implanted dopants confined in a "silicon-on-insulator" layer has yielded deeper and more uniform implant densities than had previously been possible. Preliminary results from the Goddard/Wisconsin groups show that the resulting 1/f noise per volume is at least a factor of 4 lower than previous Si thermistors, and this is just a lower limit[11] .These early results indicate that it will soon be possible to combine the advantages of working with silicon for array fabrication with the reliable doping and lower excess noise associated with the NTD thermistors.

Given a practical limit of $|a| < 6$ but a need for a few eV resolution, the total heat capacity of a semiconductor-based calorimeter must be kept below 0.1 pJ/K, making absorber selection highly constrained. Insulators and semiconductors can have impurity states in their bandgaps that trap electrons, leading to incomplete and variable thermalization. Though normal metals thermalize well, their large electronic specific heats limit their use to extremely small detectors. Semimetals such as HgTe also thermalize well, but have relatively low Debye temperatures. Superconductors with high atomic numbers and high Debye temperatures may appear attractive, but thermalization in a superconductor can be delayed by slow quasiparticle recombination times at temperatures far below the critical temperature [12] . The best performance so far has been obtained with HgTe and Sn absorbers.

The calorimeter group at the University of Milan has obtained 5.2 and 5.4 eV resolution at 5.9 keV with two calorimeters using NTD Ge thermistors and Sn absorbers[13]. These represent the best published performance of individual semiconductor-based x-ray calorimeters. The calorimeter group at the Smithsonian Astrophysical Observatory is also obtaining high performance with calorimeters made of NTD Ge and Sn absorbers [14] . For astrophysical instrumentation, however, the state-of-the-art lies with Si thermistor arrays. Micromachined arrays of ion-implanted Si with HgTe absorbers have been optimized for the 0.3 - 10 keV and < 1 keV x-ray bands respectively. The Goddard 36-pixel array flown on the Wisconsin/GSFC XQC sounding rocket experiment[15] had an energy resolution ranging from 5 to about 12 eV over the 0.05 - 1 keV band. In ground calibration, the Goddard 32-pixel XRS array [16] had resolution of 8 - 9 eV at low energies, 9 - 10 eV at 3.3 keV, and 11 - 12 eV at 5.9 keV. The array showed excellent uniformity, with less than 13% variation in resolution across the pixels. The broad band (0.4 – 12 keV) XRS instrument was part of the Astro-E observatory that was lost due to a failure of its launch vehicle on February 10, 2000. Opportunities for a reflight are under consideration. Given the progress towards reducing the 1/f noise in Si thermistors, it is likely that arrays compatible with the existing XRS spare hardware, but with improved resolution, can be produced.

Superconducting Phase-Transition Thermometers

Superconducting transition-edge sensors (TES) operate in the narrow temperature range between the normal and superconducting states of a metal film. For a TES thermometer, $|a|$ can be more than an order of magnitude higher than that of a practical semiconductor thermistor. The resistance within the transition is associated either with a normal region that grows with temperature or with the nucleation of flux channels, called phase slip lines [17] . Since most superconductors undergo their transition at temperatures too high to be of use in a microcalorimeter, it is common to use a bilayer of normal and superconducting films. Through the proximity effect, the composite film behaves as a superconductor with a lower transition temperature than the superconducting layer would have had alone. By appropriate choice of the thickness of each layer [18], the transition temperature can be tuned to the desired operating point.

The energy resolution of a calorimeter is determined by the ratio of the signal to the phonon noise and by the useful bandwidth. The use of a thermometer with higher a increases the useful bandwidth by raising both the signal and phonon noise above the white noise, improving the energy resolution for a fixed heat capacity. In the small-signal limit, for the same heat capacity, TES calorimeters will significantly outperform

semiconductor calorimeters in energy resolution.

Figure 3 – Signal, phonon noise, and Johnson noise without electrothermal feedback (as in Figure 2 and shown in dashed lines) and with a large electrothermal feedback gain (shown in solid lines).

A lower limit on the heat capacity of a calorimeter is set by the onset of non-linearity in the detector response for large temperature excursions. In both TES and semiconductor thermistors the sensitivity depends non-linearly on temperature, but for TES calorimeters there is an abrupt loss of sensitivity once the normal state has been reached. To keep the temperature excursion due to the absorption of an x-ray photon from exceeding the dynamic range of the detector, the heat capacity C of a TES calorimeter must be increased by a factor proportional to a. Since, for large values of a, the resolution scales as $\sqrt{C/\alpha}$, the fundamental limit on the energy resolution of a TES x-ray calorimeter, ~1eV, is similar to the original prediction made for semiconductor calorimeters [19]. The main advantage of a TES calorimeter lies in practical issues such as the design flexibility that a larger heat capacity budget allows. TES calorimeters can use materials with high specific heats, such as normal metals, that thermalize deposited energy quickly and efficiently, increasing the probability of actually achieving the predicted resolution.

Another advantage of the large a is the large gain of the electrothermal feedback when the TES is biased at constant voltage. This feedback enables the TES to self-regulate within its transition. Large electrothermal feedback gain makes the temperature recover faster, and it is useful to speed the recovery up to the point that the corner frequency of the thermal response matches the useful bandwidth of the device. This makes it possible to recover the temperature in a time close to the limiting thermalization and diffusion times, allowing a higher incident x-ray flux before the onset of pulse pile-up. This is important because filtering of the electrical signal can not remove the effects of pileup that result from the thermal non-linearity of a calorimeter. Figure 3 shows how electrothermal feedback suppresses the signal and the intrinsic noise terms at low frequencies.

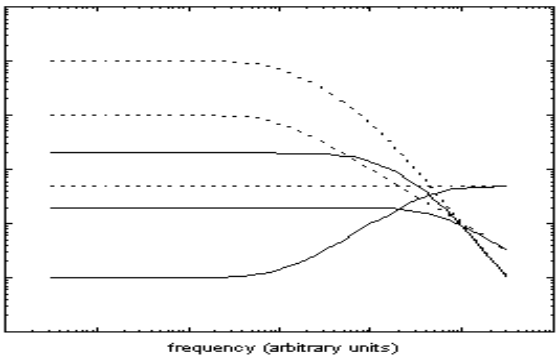

Figure 3 – Signal, phonon noise, and Johnson noise without electrothermal feedback (as in Figure 2 and shown in dashed lines) and with a large electrothermal feedback gain (shown in solid lines).

Figure 3

Just as semiconductor-based calorimeters are still being optimized in view of their non-ideal properties, excess noise in TES x-ray calorimeters is presently under investigation. Low-thermal-conductance TES bolometers made at NIST-Boulder show only the expected intrinsic noise terms, but excess current noise has been seen at both NIST and Goddard in higher-thermal-conductance x-ray devices. There is indication that this excess noise results at least in part from the nature and quality of the TES boundary conditions. More work is required before we will be able to discuss quantitatively the ultimate tradeoffs between resolution and speed.

Rapid progress has been made in improving the resolution of TES x-ray calorimeters, led by the NIST-Boulder group. They have obtained 2.0 eV resolution at 1.5 keV using an Al/Ag TES [20] and 4.5 eV resolution at 5.9 keV using Mo/Cu [21]. Recently, the Goddard group has used a Mo/Au TES to obtain 2.9 eV

at 1.5 keV and 3.6 eV at 3.3 keV for different bias points in the transition [22] . Each of these devices used a silicon-nitride membrane for the thermal isolation. Because, of the results cited, the Goddard results are the only not yet published, the 3.6 eV result is shown in Figure 4.

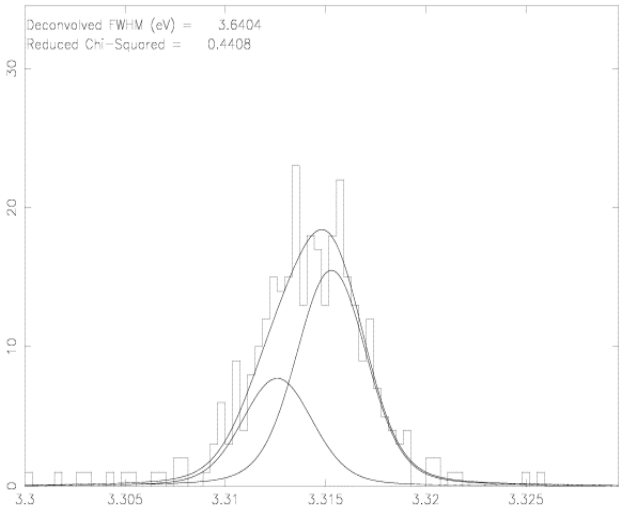

Figure 4

Magnetic calorimeters and the general case of non-resistive thermometers

There is no Joule heating, so there is no electrothermal feedback or choice of bias, in calorimeters that use thermometers not based on a change in resistance. The gain in simplicity of concept is traded against the concurrent loss of flexibility. In addition, there is no Johnson noise tied directly to the thermometric property of the sensor. (There can still be Johnson noise, as will be discussed for the specific case of the magnetic calorimeter, but it is not an intrinsic property of the thermometer.) The existence of Johnson noise made the calculation of the ultimate energy resolution of an ideal resistive calorimeter a self-contained problem. Without this intrinsic white noise source, we need to find something else, a thermalization time or another noise source, that limits the effective bandwidth.

Better than 1 eV resolution at 6 keV has been predicted for paramagnetic calorimeters. A magnetic thermometer is made of a spin system in a weak magnetic field for which there exists a small Zeeman splitting between the spin-up and spin-down energy states. When energy is deposited in the material, the amount of energy can be measured sensitively through measuring the change in magnetization using a pickup coil and a DC SQUID. Such a spin system can be realized by distributing isolated ions of d and f transition elements in a non-magnetic matrix. With $\alpha = \partial \log M / \partial \log T = -1$, the promise of these devices derives not from the size of the signal but from the intrinsic sensitivity of a SQUID [23].

Both dielectric [24] and metallic hosts have been investigated. The weak coupling between phonons and spins in a dielectric leads to very long spin relaxation times, thus metals, in which interactions with the conduction electrons speeds the spin relaxation, seem more promising host candidates [25] .
Because the sensitivity increases with the heat capacity of the spin system, the predicted resolution of an optimized magnetic calorimeter degrades more slowly with heat capacity than resistive calorimeters [26]. This feature could be an advantage for hard x-ray spectroscopy applications, for which the need for massive absorbers to stop the energetic photons is at odds with the need to minimize heat capacity.

What ends up being the bandwidth limiting noise without Johnson noise? Noise from the SQUID read-out, which is white with a 1/f component, is a major noise term. In present generation devices, it dominates the phonon noise at all frequencies. Both by improving the coupling of the signal flux to the SQUID and by reducing the read-out noise, it should be possible to reduce the SQUID noise to a level below the fundamental phonon noise at frequencies less that $1/t$. A lower limit on the SQUID read-out noise will be the intrinsic flux noise of the SQUID itself. Internal phonon noise from exchange of energy between decoupled parts of the calorimeter, for example the absorber and the thermometer or the spins and the lattice, is another potential limiting noise term [27]. Presuming the coupling is better than that of the whole device to the heat sink, this

noise is lower, per $\sqrt{Hz}$, than the fundamental phonon noise at low frequencies but rolls off at a correspondingly higher frequency. Thus, it acts as a white noise term over the measurement band. Finally, magnetic calorimeters are not exempt from Johnson noise. Johnson noise currents in a metallic absorber and nearby metal are sensed by the SQUID, and the system design must minimize this[28] .

The Brown/Heidelberg collaboration has achieved promising results using Er-doped Au [29]. In a device with a heat capacity of 1.5 pJ/K, they have attained 13 eV FWHM resolution at 6 keV. With a different device, with heat capacity of 4 nJ/K, they have measured 122 keV x-rays with 340 eV FWHM resolution. Both of these results were limited by extrinsic noise from electromagnetic pick-up and mechanical vibrations.

Conclusion

Eighteen years ago, the potential advantages of calorimetric measurement of astrophysical x-ray spectra were first realized. In that time we have moved from proofs-of-concept to space-flight instruments and from ideal theoretical detectors to a better understanding of the additional characteristics not present in the ideal detector models. The loss of Astro-E has delayed the start of the era of high-resolution, high-efficiency, astrophysical x-ray spectroscopy. The questions Astro-E would have answered are now differed to future microcalorimeter-based missions. Given the ongoing progress in the development of x-ray calorimeters, the prospects for the capabilities of future missions are quite good. This progress includes, and must continue to include, strides towards making and reading-out large arrays as well as improving the resolution and the counting rates of single pixels.

Reference

1. S. Murray, these proceedings
2. C. K. Stahle, D. McCammon, and K. D. Irwin, *Physics Today*, **52,** 32 (1999).
3. A. E. Szymkowiak, R. L. Kelley, S. H. Moseley, and C. K. Stahle, *J. Low Temp. Phys.*, **93**, 281 (1993).
4. S. H. Moseley, J. C. Mather, and D. McCammon, *J. Appl. Phys.*, (1984).
5. J. C. Mather, *Appl. Opt.* **21**, 1125 (1982) and J. C. Mather, *Appl. Opt.* **23**,584 (1984).
6. B. I. Shklovskii and A. L. Efros, *Electronic Properties of Doped Semiconductors* (Springer-Verlag, Berlin, 1984).
7. E. E. Haller, et al., these proceedings
8. J. Zhang, W. Cui, M. Juda, D. McCammon, R. L.Kelley, S. H. Moseley, C. K. Stahle, and A. E. Szymkowiak , *Phys. Rev. B*, **57**, 4472 (1998), and N. Wang, F. C. Wellstood, B. Sadoulet, E. E. Haller, and J. Beeman, *Phys. Rev. B*, **41**, 3761 (1990).
9. S. I. Han, R. Almy, E. Apodaca, W. Bergmann, S. Deiker, A. Lesser, D. McCammon, K. Rawlins, R. L. Kelley, S. H. Moseley, F. S. Porter, C. K. Stahle, and A. E. Szymkowiak, *Proc. SPIE* **3445**, 640 (1998).
10. C. K. Stahle, R.P. Brekosky, S.B. Dutta, K.C. Gendreau, R.L. Kelley, R.A. McClanahan, D. McCammon, S.H. Moseley, D.B. Mott, F.S. Porter, and A.E. Szymkowiak, *NIM A*, **436**, 218 (1999).
11. A. E. Szymkowiak, et al., these proceedings
12. A. Zehnder, *Phys. Rev. B*, **52**, 12858 (1995).
13. A. Alessandrello, J. W. Beeman, C. Brofferio, O. Cremonesi, E. Fiorini, A. Giuliani, E. E. Haller, A. Monfardini, A. Nuccioti, M. Pavan, G. Pessina, E. Previtali, and L. Zanotti, *Phys. Rev. Lett.*, **82**, 513 (1999).
14. E. H. Silver, et al., these proceedings
15. F. S. Porter, R. Almy, E. Apodaca, E. Figueroa Feliciano, M. Galeazzi, R. Kelley, D. McCammon, C. K. Stahle, A. E. Szymkowiak, and W. T. Sanders, *NIM A*, **444**, 175 (2000).
16. C. K. Stahle, M. D. Audley, K. R. Boyce, R. P. Brekosky, R. Fujimoto, K. C. Gendreau, J. D. Gygax, Y. Ishisaki, R. L. Kelley, R. A. McClanahan, T. Mihara, K. Mitsuda, S. H. Moseley, D. B. Mott, F. S. Porter, C. M. Stahle, and A. E. Szymkowiak, *Proc. SPIE*, **3765**, 128 (1999).
17. K. D. Irwin, G. C. Hilton, D. A. Wollman, and J. M. Martinis, *J. Appl. Phys.*, **83**, 3978 (1998).

18. J. M. Martinis, G. C. Hilton, K. D. Irwin, and D. A. Wollman, *NIM A*, **444**, 23 (2000).
19. K. D. Irwin, *Appl. Phys. Lett.,* **66**, 1998 (1995).
20. D. A. Wollman, S. W. Nam, D. E. Newberry, G. C. Hilton, K. D. Irwin, N. F. Bergren, S. Deiker, D. A. Rudman, and J. M. Martinis, *NIM A*, **444**, 145 (2000).
21. K. D. Irwin, G. C. Hilton, J. M. Martinis, S. Deiker, N. F. Bergren, S. W. Nam, D. A. Rudman, and D. A. Wollman, *NIM A*, **444**, 184 (2000).
22. S. R. Bandler, C. Enss, J. Schönefeld¸ G. M. Seidel, L. Siebert, and R. Weiss, *Proc. Seventh Int. Workshop on Low Temperature Detectors*, 145 (1997).
24. E. Umlauf and M. Bühler, in *Low Temperature Detectors for Neutrinos and Dark Matter IV*, ed. N. E. Booth and B. L. Salmon (Editions Frontieres, Gif-sur-Yvette, 1992), p. 229
25. S. R. Bandler, C. Enss, R. E. Lanou, H. J. Maris, T. More, F. S. Porter, and G. M. Seidel ,*J. Low Temp. Phys*., **93**, 709 (1993).
26. A. Fleischmann, C. Enss, J. Schönefeld, J. Sollner, K. Horst, J. S. Adams, Y. H. Kim, G. M. Seidel, and S. R. Bandler, *NIM A*, **444**, 101 (2000).
27. M. Bühler, E. Umlauf, and J. C. Mather, *NIM A*, **346**, 225 (1994).
28. C. Enss, A. Fleischmann, K. Horst, J. Schönefeld¸ J. Sollner, J. S. Adams, Y. H. Huang, Y. H. Kim, and G. M. Seidel, submitted to *J. Low Temp. Phys.*
29. See ref. 28.